

# Modeling heterogeneous energetic materials at the mesoscale

M.R. Baer

*Department 9100, Engineering Sciences Center, Sandia National Laboratories, Albuquerque, NM 87185-0834, USA*

---

## Abstract

The mesoscopic processes of consolidation, deformation, and reaction of shocked porous energetic materials are studied using shock physics analysis of impact on an ensemble of discrete “crystals”. This work provides a foundation for improving our understanding of the processes at the mesoscale to advance continuum-level models for energetic material performance prediction and safety assessment. Highly resolved, three-dimensional numerical simulations indicate that rapid deformation occurs at material contact points, producing large amplitude fluctuations of stress that persist over several particle diameters. Localization of energy produces “hot-spots” due to shock focusing and plastic work near internal boundaries as material flows into interstitial regions. Numerical simulations indicate that “hot-spots” are strongly influenced by multiple crystal interactions. Chemical reaction processes also induce multiple wave structures associated with particle distribution effects. This study provides new insights into the micromechanical behavior of heterogeneous energetic materials, strongly suggesting that important statistical information associated with initiation and sustained reaction in shocked heterogeneous energetic materials may be embedded in fluctuating states that are distinctly different than the single shock jump descriptions traditionally used in continuum level models. © 2002 Elsevier Science B.V. All rights reserved.

*Keywords:* Energetic materials; Mesoscale; Crystals; Hot-spots; Numerical simulation

---

## 1. Introduction

Nearly all energetic materials, including explosives, pyrotechnics, propellants, and intermetallics, are heterogeneous by nature and often consist of a mixture of polycrystalline and binder materials. These energetic mixtures exhibit distinctly different thermal/mechanical/chemical behavior than pure materials because microstructure introduces internal boundary effects at the mesoscale—the scale associated with the granular nature of the constituents in a heterogeneous energetic material mixture. For high explosives, the shock sensitivity of initiation and sustained reaction is known to be controlled by processes occurring at the crystal level [1]. For example, the threshold to reaction is greatly influenced by changes in crystal morphology, defect

content and size distribution [2,3]. Much of the current knowledge on shock-induced reaction in heterogeneous material is empirical as opposed to one based on a fundamental understanding of the underlying physical processes associated with initiation behavior.

Energetic materials are often heterogeneous mixtures that are mixed and pressed granular pyrotechnic, propellants or extrudable explosives. These materials are designed to achieve a broad range of tailored outputs, such as the delivery of a detonation signal at a prescribed time. Explosive components design usually relies heavily on the formulation of the energetic materials, with great emphasis on tailoring particle size and morphology. Some components contain critical features that are of the same size as those associated with the constituents of the energetic material. A more detailed understanding of energetic material initiation and propagation requires resolving mesoscale processes.

---

*E-mail address:* mrbaer@mailgate.sandia.gov (M.R. Baer).

At the forefront in energetic material research are new revolutionary advances in computational research and experimental diagnostics which offer new opportunities to address fundamental issues.

This paper presents computational studies at the mesoscale of granular HMX subjected to shock loading. HMX is the focus of this study because it is an extensively characterized explosive material. The ultimate goal of this work is to extend our understanding of fundamental initiation/detonation phenomena at the mesoscale to improved continuum-level models.

## 2. Prior work and technical issues

Time-resolved continuum-level measurements [4] of the shock wave structure in heterogeneous materials have provided much insight in the high strain rate processes associated with impact on heterogeneous material whereby detailed continuum-averaged particle velocities and stress fields are measured.

Fig. 1 displays the experimental configuration used to investigate the wave structure in a shock-loaded explosive layer confined between a polychlorotrifluoroethylene (Kel-F) plastic front disk and a polymethylmethacrylate (PMMA) plastic back disk. Magnetic particle velocity or polyvinylidene difluoride (PVDF) stress-rate gauges are placed on the front and back surfaces of the explosive material layer. Measurements

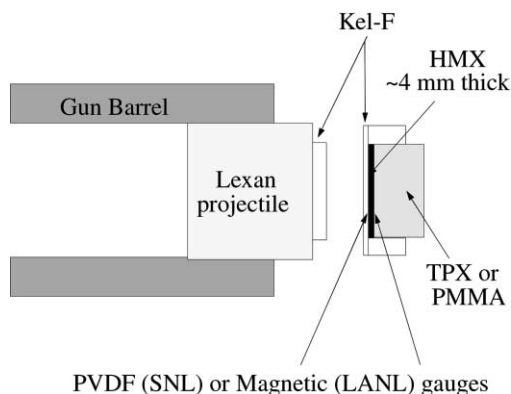


Fig. 1. Projectile and target used in shock loading experiments on porous explosive HMX.

at the interface of the Kel-F front disk and the explosive layer resolve the input loading profile, and at the interface of the back disk and explosive layer the transmitted wave profile is then determined.

The explosive powder used in these tests is a sieve-cut of HMX Holston batch HOL 920-32 having a distribution of crystals with a mean particle diameter of  $120\ \mu\text{m}$  [5]. A thin layer of crystals is packed in a 4 mm layer with a density of  $1.24\ \text{g/cm}^3$  (65% TMD) and subjected to impact loads ranging from 0.08 to 0.99 km/s (corresponding stress input of 2–25 kbar).

Fig. 2 shows an overlay comparison of particle velocity measurements to numerical calculations at

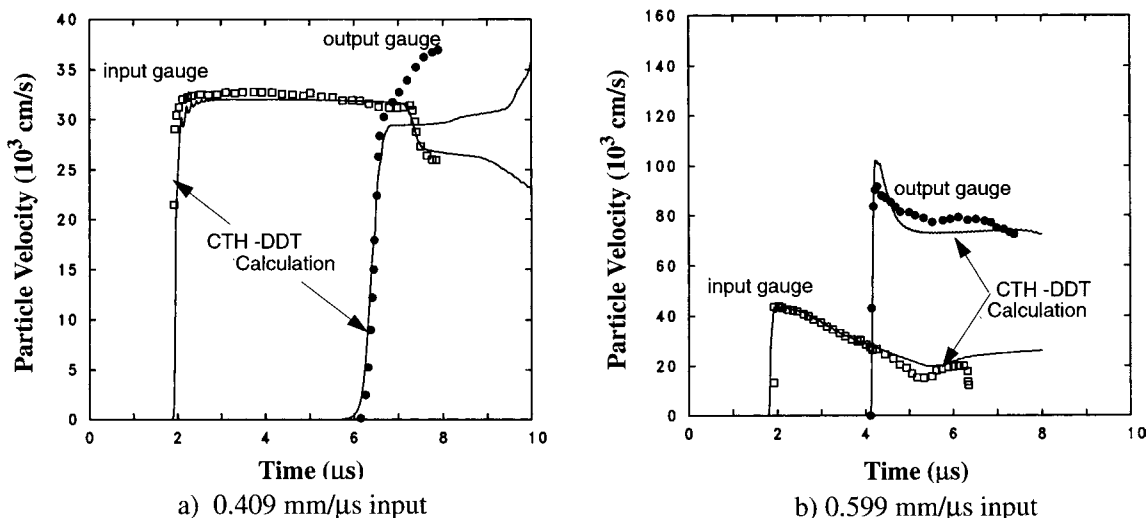


Fig. 2. Comparison of experimental and calculated wave profiles at impact conditions of (a) 4 kbar and (b) 7 kbar.

the input and output locations of the HMX layer at impact conditions of 0.409 mm/ $\mu$ s (4 kbar) and 0.599 mm/ $\mu$ s (7 kbar). (These wave fields are modeled using a continuum mixture theory [6] implemented in the shock physics code, CTH [7]. All of the details of this theory and its implementation into shock physics analysis are not repeated here, and the interested reader can find appropriate details of this information in [8,9].)

At the impact condition of 0.409 mm/ $\mu$ s, weak reaction is triggered by the compaction wave that propagates through the HMX layer and reflects off the backing surface. The finite rise time of input shock load is due to the viscoelastic response of the Kel-F front disk, whereas the dispersion in the propagated profile is the result of processes associated with compaction of the HMX powder [10]. These impact experiments suggest that the estimated thickness of the compaction wave is roughly the width of 10 particle diameters and the dispersive nature of the propagated wave is due to the concerted interaction of crystals rather than viscous flow behavior. This implies that the processes occurring within the compaction wave involve smaller length scales than can be resolved using a continuum mixture-averaged description.

At a higher loading condition of 0.599 mm/ $\mu$ s (Fig. 2b) rapid deformation at the compaction front triggers reaction in the granular HMX immediately as the wave passes through the front gauge and enters the powder. The front particle velocity decreases because the reacting HMX decelerates the cell front. Stress measurements at this experimental condition indicate that pressure continually rises, confirming that reaction is occurring. The transmitted wave amplitude grows and the wave front steepens as burning continues, and by the time the wave reaches the back of the HMX layer, the particle velocity has nearly doubled in speed. In contrast to the lower input load, a less dispersive propagated wave front is observed at the 0.599 mm/ $\mu$ s input condition.

Additional tests were conducted to study the effects of varying particle size and initial density [11]. Tests with fine grain HMX (class E), having an average particle diameter of 10–15  $\mu$ m indicate that a higher pressure threshold is needed to trigger reaction. When combustion ensues the growth of reaction is rapid due to the high specific surface area of the fine particles. In

tests with a lower HMX density, a higher degree of mechanical energy is dissipated at lower initial density resulting in greater energy localization. As one expects, this causes an increase in the shock sensitivity of the energetic material.

Although these experiments represent a significant advancement in measurement technology, these tests provide only trends of behavior, as opposed to the details of the shock loading processes. Most importantly, they reveal that the important shock processes occur in thin regions of high strain; existing measurement techniques average the response over a much larger area and are likely not resolving the important aspects of the shock behavior especially when reaction takes place.

At the crystal scale the initiation of heterogeneous materials occurs because shocks interact with material heterogeneities causing “hot-spots” that lead to reaction [1]. Localization of energy produces associated space–time fluctuations in the thermodynamic fields, such as pressure and temperature. When averaged over a sufficiently large space, these effects produce an energy release that is a combination of mechanics, dissipation, and chemistry. A variety of physical phenomena result in the creation of “hot-spots”, and it is generally agreed that plastic deformation is the dominant feature of the energy localization. This deformation is due to material rearrangement near boundaries or at internal dislocations within crystals. A theory of shock-induced “hot-spots” is based on the notion of phonon energy transport/dissipation along moving dislocations [12]. This atomic-level view, by itself, is probably too simplistic; the chemical and physical processes associated with “hot-spots” involve space–time fluctuating states at the mesoscale whereby multiple crystals interact to produce complex multiple shock and release wave structures.

Much of the current work in computational modeling of heterogeneous material describes macroscale behavior using ensemble-averaged continuum theory [6,13]. As demonstrated earlier, a continuum mixture-average approach can describe the wave fields of reactive energetic materials including initiation, growth of reaction, and reflected wave behavior. Although the formalism of continuum mixture theory remains a controversial subject in the multiphase literature, there is general agreement on the overall conservation laws [14]. Much of the disagreement

centers on the derivation of interactions associated with the exchange of mass, momentum, and energy between phases needed to provide closure to a mixture description. These interactions occur at the mesoscale associated with the discrete nature of the mixture, hence, they are included as submodels based on intuition and/or experimental guidance. Indeed, the interactive use of modeling and data has greatly assists in determining the important aspects of deformation and reaction observed in experiments. However, experimental techniques for measurement at the mesoscale crystal level are currently in development, and relatively little information is available to properly guide the formulation of micromechanical models.

At a different level of theoretical description, nonequilibrium atomistic effects can be modeled using molecular dynamics methods. Large-scale molecular dynamics solve Newton's laws of motion associated with strongly interacting atoms, and can now consider the interactions of  $\sim 10^8$  atoms to study shocks in crystalline materials. Recent efforts have revealed many remarkable aspects of these shock physics problems, such as the structure of elastic precursors/plastic waves [15] and the associated interactions with chemical reaction [16]. However, the number of atoms needed to approach the mesoscale requires a much greater computational resource than currently possible. (For example, a flake of solid material with a length scale of  $1\ \mu\text{m}$  contains  $10^{17}$  atoms; this is an insufficient fraction of material required for a mesoscale representation.) Hence, the continuum macroscale and atomistic microscale descriptions fall short of adequately describing the fundamental processes associated with reactive waves in heterogeneous media. The mesoscale has not been extensively studied; yet it is the level that bridges continuum and atomistic scales.

Detailed models of the initiation and detonation in porous energetic materials at the discrete particle level have been advanced in previous studies; a partial list of prior studies is given in [17–23]. In many of these past studies, microstructure is modeled using ordered lattices of packed circles or polygons in two dimensions. A recent work [20] treats two-dimensional microstructures generated from image processing digital photographs of granular compact cross-sections. Although this approach produces interesting pictures, the resulting descriptions are not representative of real heterogeneous systems because projection yields unrealistic

higher packing volumes and the geometric constraint of two dimensions suppresses an additional degree of freedom for material deformation. Mader and Kershner [17] were amongst the first to numerically study three-dimensional effects in shock-loaded heterogeneous energetic material. They considered a heterogeneous energetic material as a continuous media with a distributed matrix of spherical holes. Despite limitations of computational resources and inadequate mesh resolution, their numerical simulation produced gross features of the wave propagation behavior associated with pore collapse. However, realistic granular descriptions usually consist of mixed materials with different properties, and the interactions of crystal boundaries, including the effects of sliding contact surfaces and pore collapse, are considered important aspects of wave behavior.

Shock physics analysis currently has the resources of parallel computing architectures to provide enhanced resolution of shock processes in heterogeneous material descriptions that closely represent realistic material configurations. The following study presents three-dimensional simulations of shock impact on an ensemble of polycrystalline explosive and binder materials. Detailed wave fields are presented to illustrate the richness of wave phenomena associated with the effects of material strength, thermal dissipation and reaction on the shock-loading behavior at the mesoscale. The results of the current work are based on simplistic material descriptions with the intent to provide an introduction to the current capabilities of mesoscale modeling, including its uncertainties and shortcomings, to motivate the need for improved material descriptions and experimental diagnostic tools.

### 3. Crystal morphology

Fig. 3 displays photo-micrographs of HMX (octahydro-1,3,5,7-tetranitro-1,3,5,7-tetrazocine); TATB (2,4,6-trinitro-1,3,5-benzenetriamine) and PETN (2,2-bisnitroxymethyl-1,3-propanediol, dinitrate) crystals which are common explosive crystals used in plastic-bonded explosives (LX's and PBX's). Crystalline explosives are embedded in curable or polyadditiveplastics, such as polyurethane, chloro-fluor-polymer, silicon resin, nitrocellulose, etc. to produce an elastic or rubbery

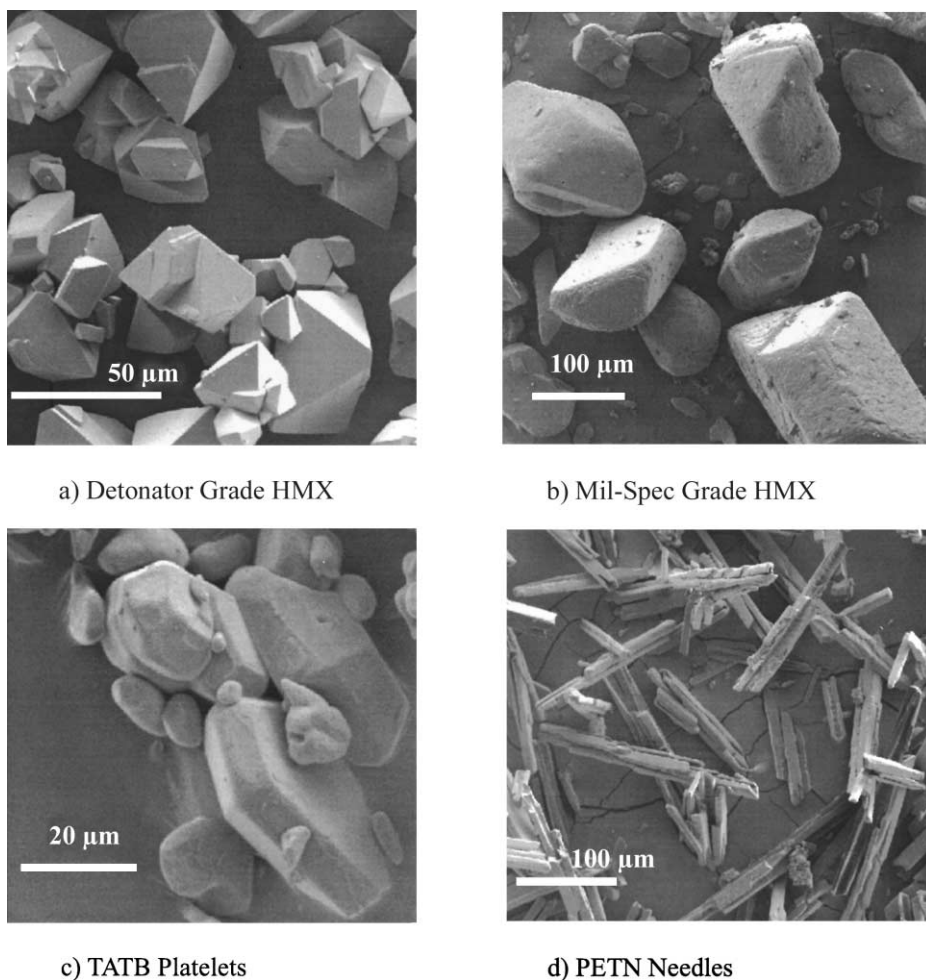


Fig. 3. Various crystal morphology for typical explosives materials: (a) detonator grade HMX; (b) mil-spec grade HMX; (c) TATB platelets; (d) PETN needles.

material that can be pressed, moulded, or machined to a desired shape.

HMX is a well-characterized explosive polycrystalline material that is often mixed with binders to produce a high output explosive charge. Fig. 3a and b show two different grades of class D HMX having similar mean particle size and morphology. Detonator-grade HMX has a crystal morphology with edges that are sharper than those of mil-spec HMX. A slight variation of crystal shape leads to different initiation characteristics, and the smoothing of material boundaries is known to reduce the shock sensitivity of the explosive [2]. In addition to external boundaries, optical microscopic images reveal that crystals contain

internal defects, such as gas or solvent-filled inclusions [3]. These internal boundaries are possible sites for energy localization.

Fig. 3c displays TATB crystals having a plate-like morphology. TATB is a common ingredient in insensitive high explosives such as PBX-9502 (95% TATB and 5% Kel-F). Another common explosive ingredient is PETN (shown in Fig. 3d) which has needle-like morphology. This explosive material is formulated with binder materials to produce XTX-8003 (80% PETN and 20% Sylgard) commonly used as a sheet explosive. As illustrated in this figure, a wide variety of crystal morphologies are encountered in the field of energetic materials.

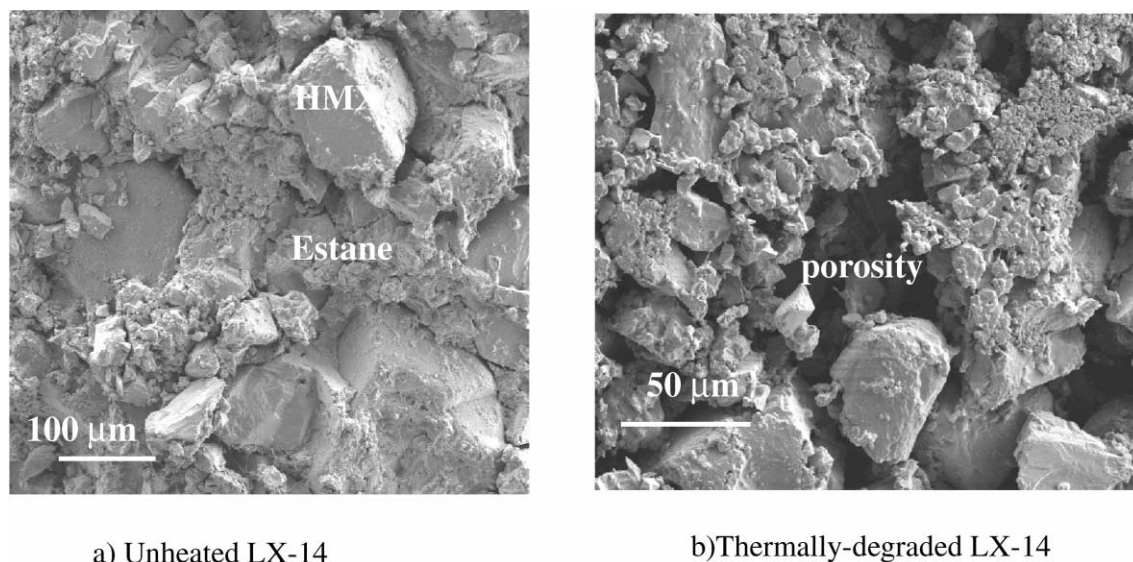


Fig. 4. Photo-micrographs of (a) unheated and (b) thermally-degraded LX-14.

A photo-micrograph of LX-14 (95.5% HMX, 4.5% estane) is shown in Fig. 4 to illustrate the microstructure of typical crystal/binder systems. In its virgin state the binder material fills the interstitial regions with granular-like nodules (blended material also contains a few percent of porosity). As these materials age or are subjected to abnormal thermal–mechanical environments, changes in the microstructure greatly alter the performance and initiation characteristic of the energetic material. Fig. 4b shows a photo-micrograph of LX-14 that has been confined and heated to 40 °C for 20 min. Quasi-static measurements indicate that stress is relieved as the binder softens, and crystals debond from the binder material forming large regions of open porosity [24]. In addition to binder migration, phase change in the crystalline HMX produces cracks as a result of changes in crystal density [25]. When HMX is heated, thermal decomposition leaves a residual with shell-remnants because of the release of gaseous products within trapped bubbles [26].

Fig. 5 shows a scanning electron microscopy (SEM) image of a thermally degraded HMX crystal with the residue morphology produced by decomposition. If reaction is triggered in this material, thin flames can penetrate into microcracks to induce convective burning which self-accelerates to support shocks and the onset of deflagration-to-detonation transition (DDT).

This thermally damaged microstructure most likely causes rapid flame spread which greatly influences the degree of reaction violence during a cookoff event [27].

Similar changes in microstructure may occur as an energetic material ages. Fig. 6 shows photo-micrograph

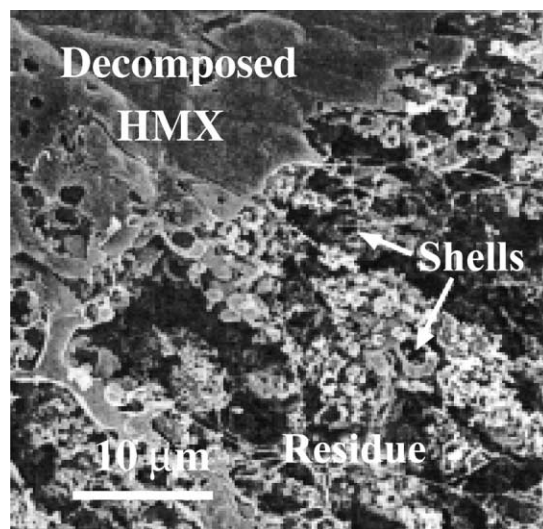


Fig. 5. SEM of a thermally degraded crystal of HMX showing the detailed structure and morphology of the decomposed energetic material.

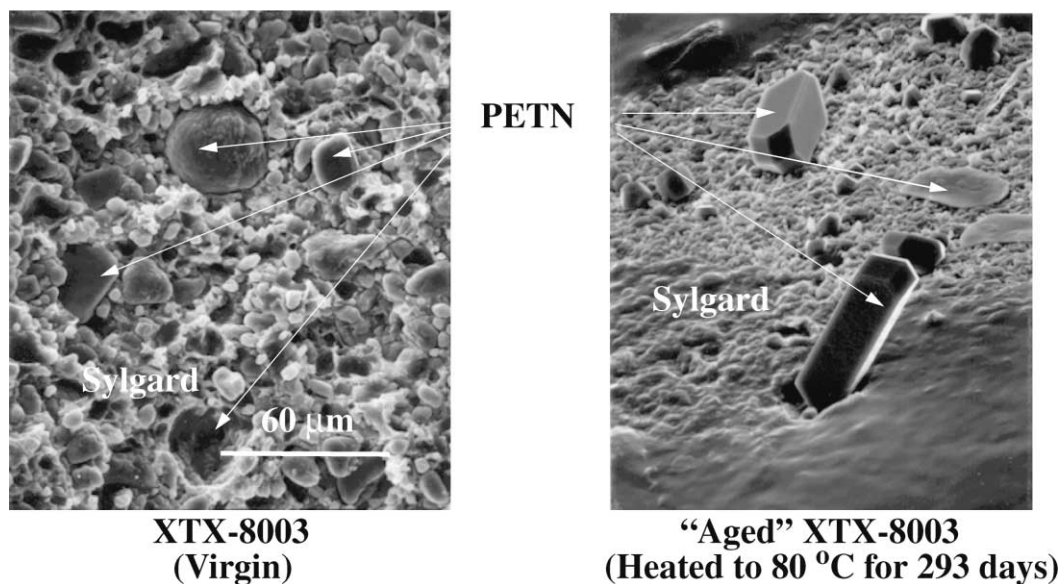


Fig. 6. Photo-micrograph of virgin and “aged” XTX-8003.

of XTX-8003 that has been “aged” by heating the material to 80 °C for 293 days [28]. In virgin material the PETN and Sylgard binder consist of a mixture of spherical-like particles. As the material ages, segregation of material takes place; large PETN crystals form and migrate to open porosity leaving regions with material nonuniformity or additional void. The interplay between chemical and structural stability is not well understood at this time and little information is available regarding these ageing effects.

In the section to follow, an approach is introduced to study the effects of microstructure on impact behavior of heterogeneous materials. Although new experimental methods are being advanced to resolve physical phenomena of shock-loaded material at crystal length scales and nanosecond time resolution, this work centers on direct numerical simulations to investigate the highly transient wave fields at the mesoscale. It is shown that “shock” fronts in heterogeneous materials consist of multiple waves producing space–time fluctuations of stress and energy that are distinctly different from the classical view of shocks. The statistical nature of these organized wave structures is likely a key feature for gaining a better understanding the role of microstructure on wave behavior. It is hoped that this improved description

of shock-loaded material behavior leads to better models for detonation in heterogeneous media and insights for improving performance and safety of energetic materials.

#### 4. Mesoscale modeling

Three-dimensional shock wave structures in heterogeneous materials are investigated using the Eulerian CTH shock physics code [7] for a mixture of “crystals” and binder having multimaterial disordered geometry and several relevant aspects of material physics. Although most polycrystalline materials are known to have structural regularity and directional-dependent material properties, this work considers materials with idealized morphology and isotropic properties.

In constructing a material configuration, the statistical nature of the heterogeneous media is represented by a computational geometry describing an ensemble of “crystals” with varied size distribution consolidated to a random, closely packed configuration. In real energetic materials a myriad of crystal shapes are encountered, however, this work considers the shock behavior for a collection of “crystals” with polyhedral geometry.

To generate a random packing of arbitrary polyhedral “crystals”, several strategies have been considered. Initially, a drop-and-fill method was used whereby an arbitrary number of spherical particles is introduced into a random space, and the rigid body motion, under the influence of “gravity”, leads to interbody collision and contact frictional effects [29]. Unfortunately, this produces a stereological system with a directional bias and nonuniformities near boundaries; thus an alternative strategy was sought.

A more efficient means of generating a random ensemble of particles is based on the statistical mechanical theory of liquids [30,31]. In this approach, Monte Carlo (MC) and molecular dynamics (MD) methods are used to generate closely packed particles of arbitrary distributions. As illustrated in Fig. 7, a large region of three-dimensional space is filled by placing a specified number of particles on the lattice sites of a simple cubic array. The particle size is chosen randomly from a prescribed discrete distribution. The starting packing fraction is chosen to be sufficiently low such that the initial configuration is free of any particle overlap. The particles are then given random velocities, and a molecular dynamics simulation is conducted using a standard collision algorithm. Given the low packing fraction, the initial lattice configuration quickly disintegrates and evolves to a low-density, equilibrated fluid mixture. This equilibrium configuration forms the starting point for an efficient densification MD simulation in which the density is increased dynamically until the particles

are essentially locked in place. The densification algorithm employs growing particles whose size increases at a constant rate, while the particles continue to move through space and undergo collisions. The MD simulation continues until the packing configuration reaches a specified target volume fraction or a maximum packing condition.

The ensemble of crystals are chosen to have the properties of HMX with an unpressed particle size distribution for Holston lot 920-321. Closely packed configurations are determined using the MC/MD method considering five classes of particle sizes (fine particles are lumped into the smallest size category). In applying the packing algorithm, the ensemble of HMX “crystals” reaches a closely packed limit density of approximately 65% TMD. (To achieve higher densities, mechanical deformation/fragmentation of the “crystals” takes place or, alternatively, interstitial regions are filled with binder.)

As a model simplification isotropic properties are used to describe the crystalline HMX material. To maintain separate identities for each particle size category, unique material numbers are assigned with common is equation of state and material strength descriptions. By this means, interactions of material boundaries can be accommodated. Material boundary interactions are treated by imposing mixing rules for the yield strength within computational cells containing material interfaces. A frictionless material interface is represented by imposing a zero material yield in mixed-material computational cells. Alternatively a

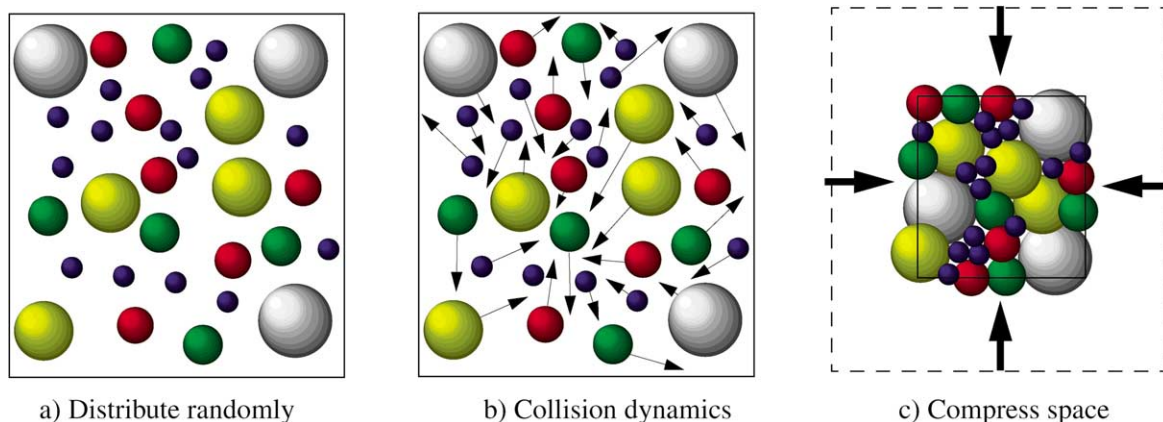


Fig. 7. Pictorial of the MC/MD method used to create a closely packed ensemble of “crystals”.



Table 1  
 HMX EOS/strength/fracture parameters

Parameter	Value
Particle size distribution ( $\mu\text{m}$ )	Weight fraction
<44	0.092
62	0.121
88	0.118
125	0.278
177	0.182
250	0.156
>350	0.053
Crystal density— $\rho_0$ ( $\text{g}/\text{cm}^3$ )	1.9
Sound speed— $c_0$ ( $\text{cm}/\text{s}$ )	$2.74 \times 10^5$
Slope of $U_s-U_p$ Hugoniot— $s$	2.6
Grüneisen parameter— $\Gamma_0$	1.1
Specific heat— $c_v$ ( $\text{erg}/\text{g EV}$ )	$1.45 \times 10^{11}$
Yield stress— $Y$ (kbar)	1.0
Poisson ratio— $\nu$	0.25
Fracture stress— $\sigma_f$ (kbar)	-20.0

volume fraction-weighted yield strength constraint produces material interfaces that are continuously bonded. A Mie–Grüneisen equation of state is used for the HMX hydrodynamic response and an elastic–perfectly plastic model, with yield at 1 kbar, is included for deviatoric stresses. A list of model parameters is given in Table 1 [32].

In the first set of calculations shown in Fig. 8, inert HMX “crystals” are impacted at 1000 m/s. Although it is recognized that the induced stress levels are sufficiently high to trigger reaction, the focus of the calculation centers on the thermal–mechanical behavior without the complication of chemical reaction. Thermal conduction effects are also included in these simulations since the competing effects of energy localization and dissipation ultimately dictate the onset of reaction.

Periodic lateral boundary conditions are placed on the computational domain, and at the impact boundary a hard wall condition is imposed. A reverse-ballistics calculation is represented by material stagnating at the boundary. This produces multiple shocks that pass back into the “crystal” array. The resolution of these calculations, using a uniform  $5 \mu\text{m}$  cell size, requires well over 27.5 million computational cells. Fig. 8 displays a midplane cross-section of the material interfaces, pressure, and temperature contours for

three, 200 ns intervals after a 1000 m/s impact. The simulations display the details of the rapid deformation occurring at material contact points. The nature of the dispersive fields includes large amplitude fluctuations of stress with wavelengths of several particle diameters. These fluctuating fields occur because of the effects of shocks interacting with individual material surfaces and multiple crystal interactions. Interestingly, the amplitude of the fluctuating pressure field is of the same order as the mean pressure state.

Localization of energy produces “hot-spots” owing to shock focusing and plastic work as material flows into interstitial regions. The effect of thermal dissipation leads to a decay of the “hot-spot” temperatures. It is the race between energy localization and dissipation that dictates the initiation and sustaining of reaction. Numerical simulations demonstrate that the “hot-spots” scale directly to particle size which suggests that the character of the preshocked material establishes the statistical nature of the energy localization. It is noted that crystals usually possess anisotropic properties [33] and contain internal defects [3], which may also alter the distribution of “hot-spots”.

As a comparative numerical simulation, impact on plastic bonded material is modeled with the HMX “crystals” and polyurethane binder (shown in Fig. 9). Here, the interstitial regions are filled with the polymeric binder containing a small volume fraction of randomly dispersed voids. In this example, a void volume fraction of  $\sim 5\%$  is incorporated in the binder material. An elastic–perfectly plastic material strength model is applied with a yield stress of  $\sim 0.1$  kbar and a Poisson’s ratio of  $\sim 0.45$ . As in the prior calculation, all material interfaces are treated as frictionless. The material surfaces are displayed along with midplane contours of temperature and pressure at 100 ns intervals after impact. In this example, multiple shocks arise that move at nearly twice the velocity of that seen in the prior HMX simulation because of the higher density of material. Since the pores are filled with polyurethane and voids, the shocks pass through material interfaces having different shock impedance characteristics, and multiple waves coalesce and release as the crystals interact with themselves and with the binder.

As the shocks interact with the voids, pore collapse produces jets that penetrate into adjacent “crystals”. As one would expect, much of the material distortion

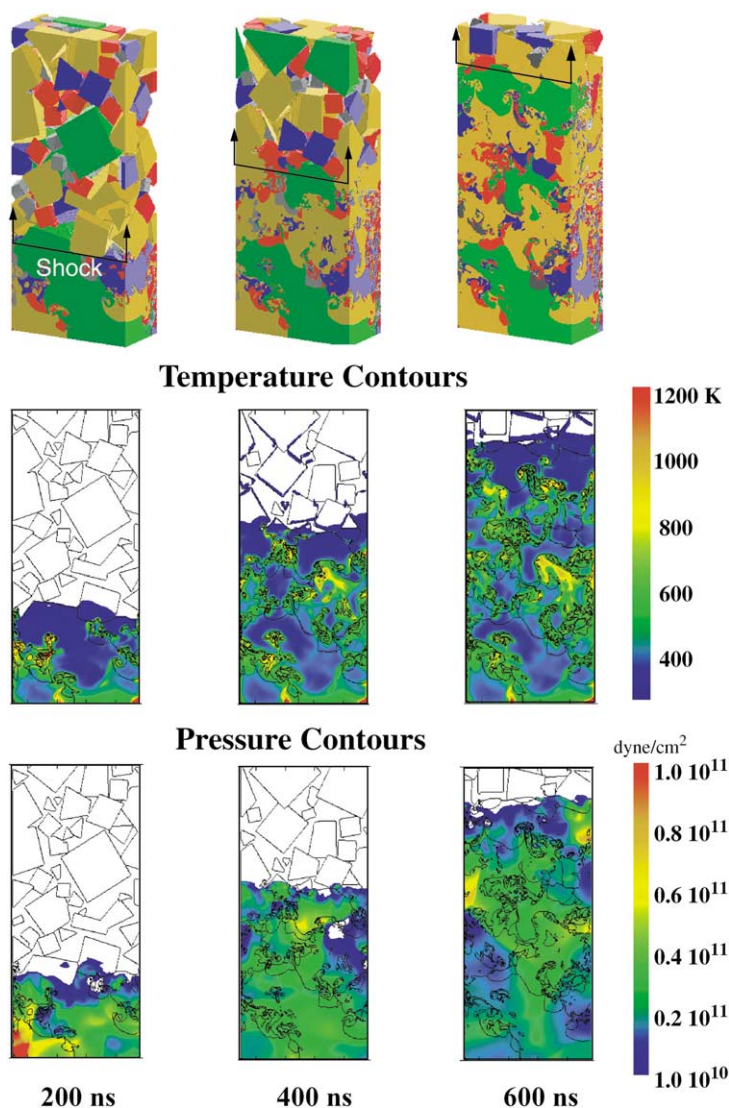


Fig. 8. Midplane cross-sectional contours of a 1000 m/s impact on HMX Holston 920-32.

occurs in the binder material; however, the effect of shock focusing and jetting into the HMX crystals is evident. Again, the stress field exhibits fluctuations and nonequilibrium behavior and patterns of wave coalescence and rarefaction associated with the multiple waves having Mach stems and nonplanar fronts. To better illustrate the localized heating in the energetic material the temperature contours for only the HMX material are shown in Fig. 10. Localized regions of high temperature are clearly seen at the locations

where pore collapse and jetting into individual crystals occur.

To investigate the effect of crystal shape, simulations are conducted for a 1000 m/s impact on an ordered array of single size (100  $\mu\text{m}$ ) HMX, approximated as spheres or cubes with random orientation. In contrast to smoothed particle surfaces, the effects of angular morphology are assessed. Lagrangian tracer points are included at the center of each HMX “crystal” along the centerline. At these locations, the

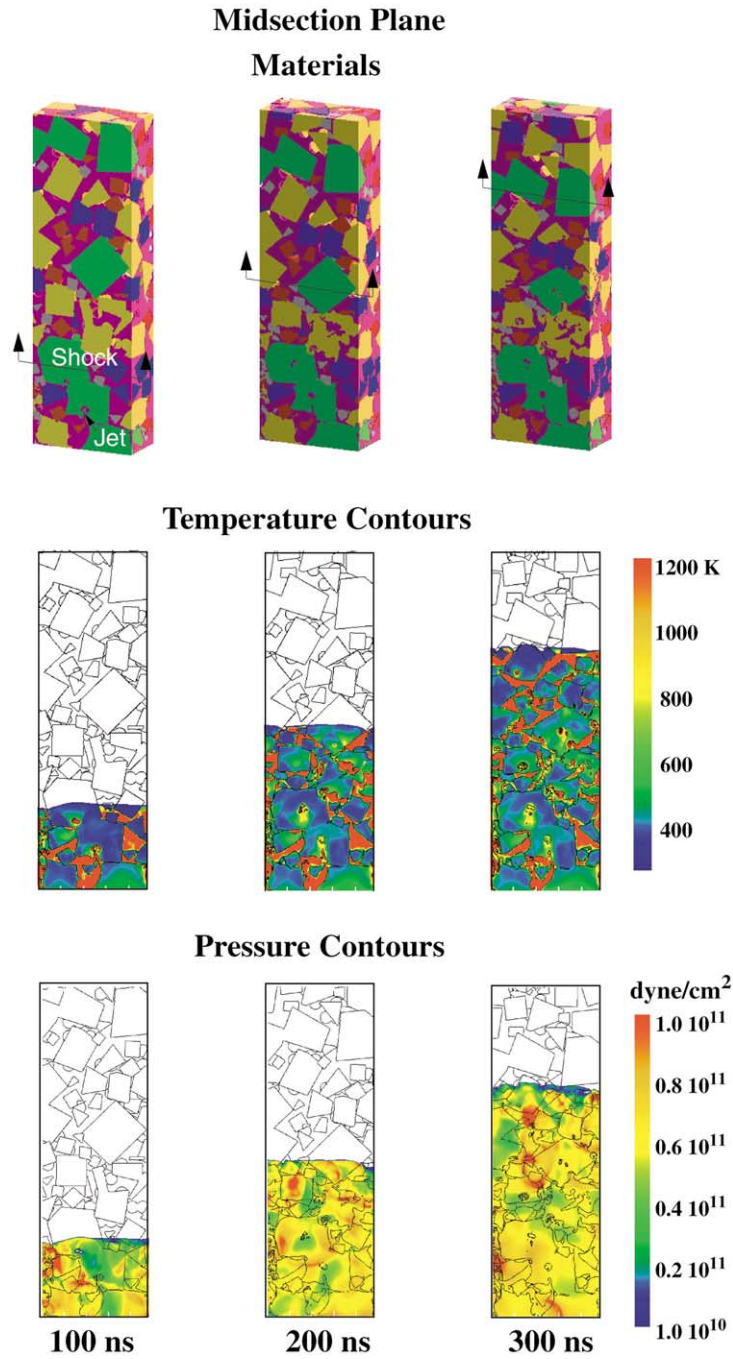


Fig. 9. Midplane contours of a 1000 m/s impact on HMX with a polyurethane binder and 5% porosity.

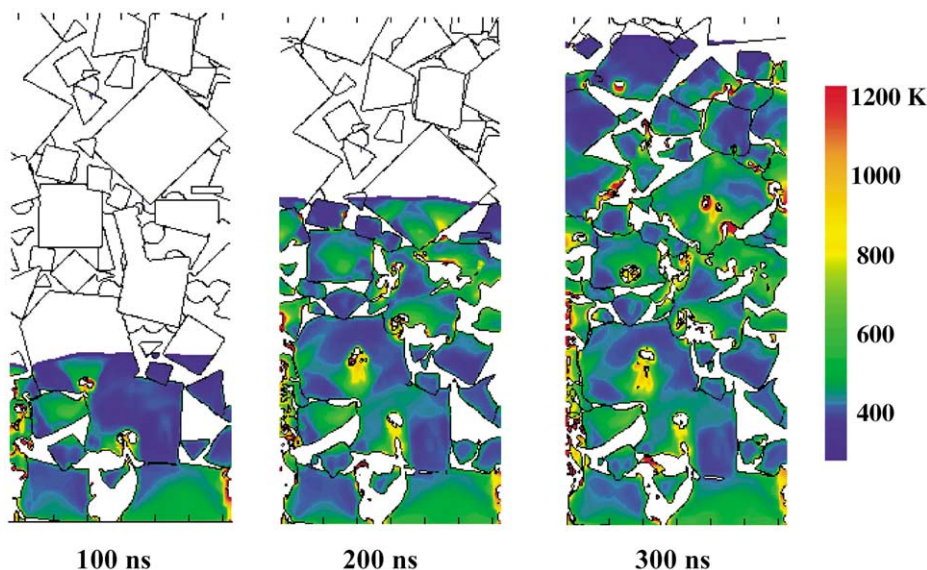


Fig. 10. Temperature contours in the HMX crystals showing localized heating effects owing to jetting associated with pore collapse.

stresses are monitored and an overlay of the centerline pressure histories are given in Fig. 11. As seen in these simulations, fluctuating fields are due to the effects of shocks interacting with individual material surfaces and contact points.

In this calculation, the mean pressure field is  $\sim 40$  kbar, and the amplitudes of the shocks traversing the “crystals” are of the same order. These highly fluctuating stress states persist over several particle diameters. The pressure histories of the ordered spherical particles exhibit higher pressure fluctuations than the cubic system because of resonance. As one might expect, disorder of particle orientation reduces the resonant effect.

## 5. Mesoscale reactive model

In the previous section, numerical simulations considered only thermal and mechanical effects without the effect of reaction. At the 1000 m/s impact condition, the localized temperatures are seen to exceed those required for prompt reaction. An appropriate model for chemistry that would be used to assess reaction induced by localized heating must include multistep endothermic and exothermic mechanisms similar to those proposed by McGuire and Tarver [34]

and kinetics rate data, such as measured in diamond anvil studies by Russel et al. [35]. Multistep chemistry with multiphase states, similar to those used in finite element analysis [36], is currently being implemented in shock physics analysis.

In the absence of a more physically relevant reaction model, we have applied an ignition/growth two-state history variable reactive burn (HVRB) model [37]. In this approach, reaction is triggered at a pressure threshold (as opposed to a temperature criteria) and a pressure-dependent rate law describes the extent of reaction. This single reaction progress variable description has generally led to good agreement with experimental run-to-detonation pop-plot and other data at the continuum-level. Thus, the application of this approach assumes that all reaction pathways are self-similar to averaged state data. Utilization of this model approach provides preliminary insight into what can be expected when more physically based combustion descriptions are determined for the crystalline HMX.

In the following example, a numerical simulation is shown with a spatial extent that bridges the mesoscale to the macroscale. In this calculation, about 1900 HMX crystals are impacted by a copper flyer plate at 1000 m/s, and reaction is triggered by the HVRB model. Reaction parameters are set for short run

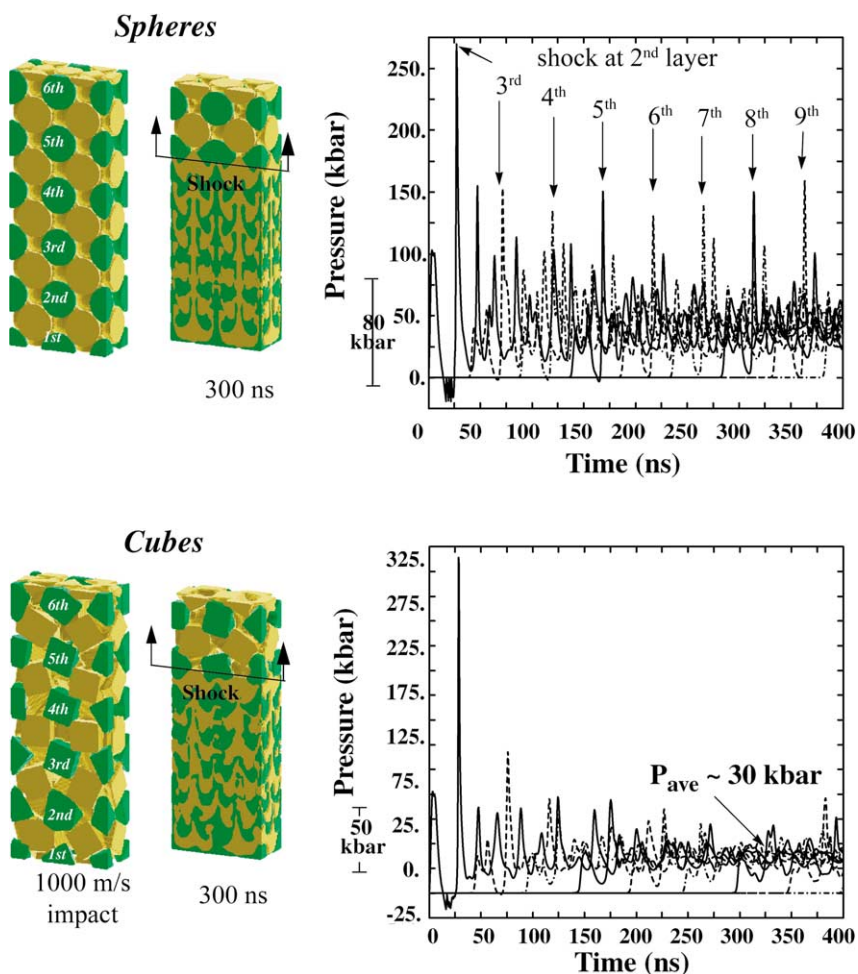


Fig. 11. Stress histories along the centerline of the nonreactive HMX crystal array modeled as ordered spherical particles (upper) vs. randomly oriented cubes (lower) of size  $100\ \mu\text{m}$ .

distance-to-detonation in order to explore the nature of the detonation wave through the random crystal structure.

Fig. 12 displays a computational space defined by about 12 million, evenly-spaced,  $5\ \mu\text{m}$  cells. The crystal array considers the HMX Holston 920-32 particle size distribution packed to a 68% TMD density. (A dime-sized sample of 190,000 crystals resolved with 1.3 billion cells required using the entire Sandia TFLOP parallel computer with 4500 processors and 104 MB processor.)

To display the transient initiation and growth of reaction at the grain scale, it is convenient to display

several cross-sectional cut planes of pressure contours at various times. Fig. 13 displays the  $x$  and  $z$  planes at times 10, 30 and 50 ns after initial contact with the copper impactor plate. It is noted that spatial fluctuations also occur in directions normal to these two-dimensional surfaces.

In the upper time sequence of contour plots, initiation of rapid reaction is seen to first occur in the large “crystals”. Lower sustained stresses occur in smaller particles due to rarefaction effects at grain surface boundaries. As the reactive wave proceeds from crystal-to-crystal, coalesced shocks produce Mach stems. These shocks interact with grain boundaries, and as



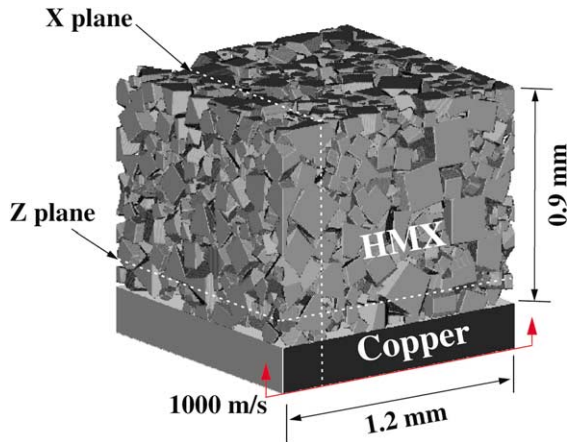


Fig. 12. HMX crystal array and 0.2 mm thick copper plate impacting at 1000 m/s.

the reaction nears completion, they merge and the wavelength of the localized stress field grows in spatial extent. In this simulation, localized pressures exceed 400 kbar. Clearly, the detonation wave struc-

ture of reactive heterogeneous materials is far more complex and greatly different than that based on singular state analysis.

## 6. Future directions in experiments and modeling

As discussed earlier, a better understanding of the shock processes at the mesoscale requires new experimental methods having the time and space resolution to capture the fluctuating fields occurring at the crystal level. Recently, a new measurement technique has been explored at Sandia National Laboratories to provide spatially resolved particle velocity in shock-compressed heterogeneous materials. Velocity interferometry is a well-established and frequently used method to obtain velocity time history during shock loading [38,39]. In contrast to the particle velocity magnetic gauge diagnostics, used in the earlier gas-gun tests, the optical velocity measurement is noninvasive and offers greater time and spatial resolution. Recently, significant progress has been made to mod-

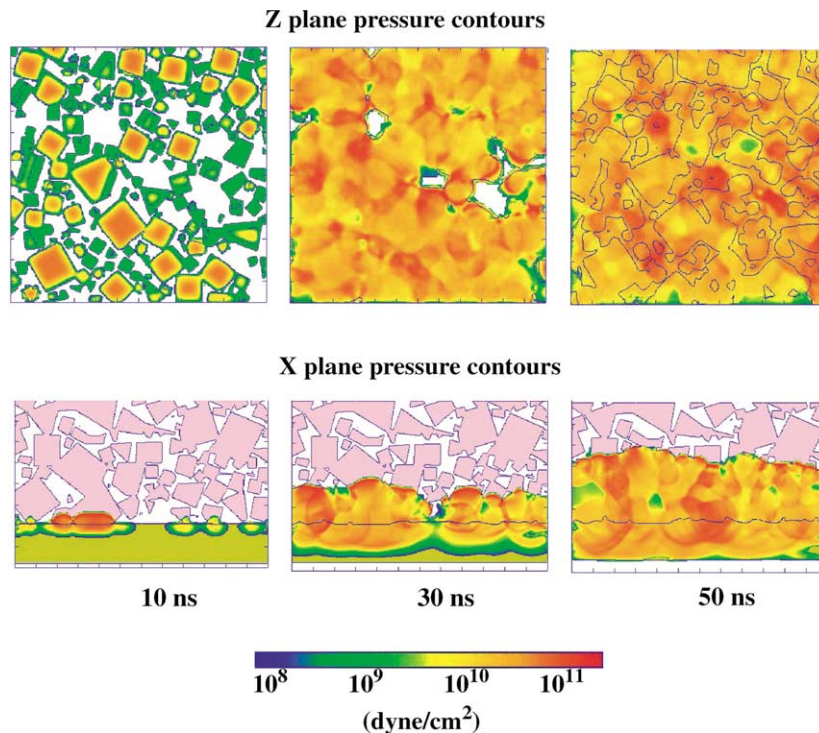


Fig. 13. Transient structure of mesoscale detonation wave growth and propagation in 68% TMD HMX.

ify an optically recording velocity interferometry system (ORVIS, [39]), producing a line-imaged interferometer with a time resolution of the order  $\sim 3$  ns and a spatial resolution of  $\sim 3$   $\mu\text{m}$ . This technique offers much promise in determining mesoscopic effects during shock loading. The details of this technique are not repeated here, and the interested reader can find this information in [40].

As a demonstration of this new capability, the thin granular layer impact experiments were repeated using the VISAR and line-ORVIS techniques. Rather than using an energetic material these tests investigated inert sugar simulant material to avoid the complications of reaction. Fig. 14 shows typical particle velocity measurements at an impact condition of 0.5 km/s which replicate measurements observed earlier using magnetic particle velocity gauges. The VISAR produces a continuum level waveform measurement whereas the line-ORVIS given on the right produces detailed wave structures. Beyond illustrating the potential for finely resolved measurements, these preliminary tests provide conclusive proof that fluctuating states are a very real aspect of the shock behavior. This new experimental technique opens many possibilities in exploring heterogeneous material behavior.

An ultimate goal of the mesoscale modeling is to provide detailed information on thermal/chemical/mechanical behavior to quantify localization effects. The procedures for interrogating extensive data of three-dimensional numerical calculations and manip-

ulating fields to link the mesoscale information to continuum-based models involves manipulating massive quantities of information. All of the difficulties tied to the modeling also apply to unraveling the detailed wave measurements obtained from the line-ORVIS technique.

As an illustration of the magnitude of this information transfer problem, consider a simulation using 1 billion cells, each cell containing 10 field variables per time step. Typically, thousands of time steps are conducted in shock physics analyses, so extracting the detailed information means manipulating a system containing  $10^{13}$  history data points. When translated to database requirements, one is faced with dealing with hundreds of gigabytes from a single simulation. Ensemble averaging then requires manipulating many simulation data sets which totals to terabytes of information! Clearly, post-processing of the detailed data from massively-parallel computations is not a trivial exercise. Future work is being directed to address these data transfer issues to provide a capability for linking mesoscale modeling to continuum descriptions.

Ultimately, the mesoscale measurements and modeling can be merged to determine the statistical properties of thermodynamic and mechanical states during shock loading which can be related to macroscale fields or to characteristics of the undisturbed heterogeneous material. Although much prior work has focused on determining probable energy localization “hot-spot” mechanisms, very little information on the

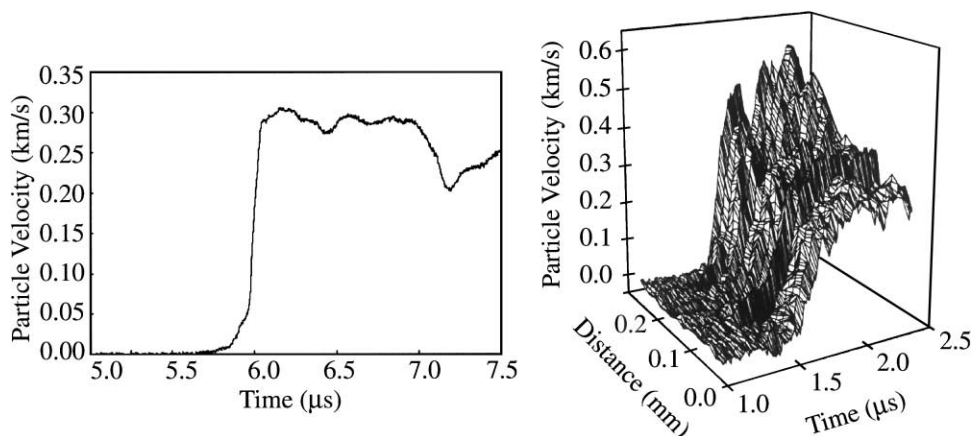


Fig. 14. VISAR (left) and ORVIS (right) records of the particle velocity associated with propagated compaction waves in granulated sugar.

statistical nature of the “hot-spots” has been obtained, yet it is this statistical nature that is most critical in developing improved and predictable models for shock initiation of heterogeneous reactive materials. Early experiments tried to determine this statistical information using time-resolved infrared radiometry [41] or optical emission techniques [42] with only marginal success. Hopefully, new measurement technology [40,43,44] can be applied to heterogeneous reactive materials to provide detailed information on mesoscale behavior.

## 7. Summary and conclusions

This study has focused on providing detailed wave information needed to define the appropriate length and time scales for new measurement techniques that may lead to a better understanding of the processes associated with mechanical initiation of granular energetic materials. Continuum mixture modeling has been successfully applied to replicate impact measurements; however, these ensemble-averaged models are inadequate and do not currently include descriptions of the highly transient fields near shock fronts. These effects may be the key to describing shock initiation of heterogeneous materials. Work is in progress to apply averaging methods and data interrogation techniques to the extensive numerical data from mesoscale simulations to determine constitutive models that can then be used in continuum descriptions.

Mesoscale modeling has been applied to the study of dispersive waves experimentally observed in prior reported work. Detailed shock physics analyses reveal that the shocked heterogeneous materials exhibit highly fluctuating stress states and the localization of energy owing to plastic deformation and crystal interactions. This modeling suggests that the shock waves (or even detonations) in heterogeneous materials are not single jump states and the structure of these wave is rich with statistical information that may key to understanding the processes associated with the initiation and growth of reaction. Future modeling is planned to investigate the effect of defects within crystals (such as voids or shear bands), blends of material (such as metals) and improved material strength, interface interactions and reaction models.

## Acknowledgements

I would like to thank M. Kipp (SNL) for help with the computational work and F. van Swol (SNL) for assistance in the MC/MD modeling. I also thank Anita Renlund (SNL) for providing many of the microphotographs of the explosive materials and Wayne Trott (SNL) for sharing experimental results from the line-ORVIS impact experiments. The many fruitful discussions with R.A. Graham (SNL), S. Sheffield (LANL), C. Tarver (LLNL) and C.O. Leiber (WIWEB) are also gratefully acknowledged. This work was performed at Sandia National Laboratories, a multiprogram laboratory operated by Sandia Corporation, a Lockheed-Martin Company, for the United States Department of Energy under contract DE-ACO4-94AL85000.

## References

- [1] F.P. Bowden, A.D. Yoffe, *Initiation and Growth of Explosions in Liquids and Solids*, Cambridge University Press, Cambridge, 1952.
- [2] A.C. Van der Steen, H.J. Verbeek, J.J. Meulenbrugge, in: *Proceedings of the 9th Symposium (International) on Detonation*, Portland, OR, 1989, p. 83.
- [3] L. Borne, in: *Proceedings of the 10th Symposium (International) on Detonation*, Boston, MA, 1993, p. 286.
- [4] S.A. Sheffield, R.L. Gustavsen, R.R. Alcon, R.A. Graham, M.U. Anderson, in: S.C. Schmidt, J.W. Shaner, G.A. Samara, M. Ross (Co-Editors), *Proceedings of High-Pressure Science and Technology*, Colorado Springs, AIP Press, New York 1994, p. 1377.
- [5] J.J. Dick, *Combustion Flame* 54 (1983) 121.
- [6] M.R. Baer, *High-Pressure Shock Compression of Solids. IV. Response of Highly Porous Solids to Shock Loading*, Springer, Berlin, 1996 (Chapter 3).
- [7] J.M. McGlaun, S.L. Thompson, M.G. Elrick, *Int. J. Impact Eng.* 10 (1990) 351.
- [8] M.R. Baer, J.W. Nunziato, *Int. J. Multiphase Flow* 12 (1986) 861.
- [9] M.R. Baer, E.S. Hertel, R.L. Bell, *Shock Compression of Condensed Matter*, Seattle, WA, 1995, American Institute of Physics, NY, 1996, p. 433.
- [10] M.R. Baer, R.A. Graham, M.U. Anderson, S.A. Sheffield, R.L. Gustavsen, in: *Proceedings of the JANNAF Combustion and PSHS Joint Meeting*, Monterey, CA, 1996.
- [11] S.A. Sheffield, R.L. Gustavsen, M.U. Anderson, *High-Pressure Shock Compression of Solids. IV. Response of Highly Porous Solids to Shock Loading*, Springer, Berlin, 1996 (Chapter 2).
- [12] C.S. Coffey, in: *Proceedings of the 10th Symposium (International) on Detonation*, Boston, MA, 1993, p. 824.



- [13] D.A. Drew, S.L. Passman, *Theory of Multicomponent Fluids*, Springer, Berlin, 1998.
- [14] D.S. Drumheller, *Int. J. Eng. Sci.* 38 (2000) 347.
- [15] B.L. Holian, P.S. Lomdahl, *Science* 280 (1998) 2085.
- [16] C.T. White, D.H. Robertson, D.R. Swanson, M.L. Elert, in: *Proceedings of the 1999 APS Conference on Shock Compression of Condensed Matter*, Snowbird, UT, 1999, p. 377.
- [17] C.L. Mader, J.D. Kershner, in: *Proceedings of the 9th Symposium (International) on Detonation*, Portland, OR, 1989, p. 693.
- [18] R.L. Williamson, *J. Appl. Phys.* 68 (1990) 1287.
- [19] D.J. Benson, W.J. Nellis, in: S.C. Schmidt, J.W. Shaner, G.A. Samara, M. Ross (Co-Editors), *Proceedings of High-Pressure Science and Technology*, Colorado Springs, AIP Press, New York, 1994, p. 1243.
- [20] D.J. Benson, P. Conley, *Modeling Simulations Mater. Sci. Eng.* 7 (1999) 333.
- [21] S.G. Bardenhagen, J.U. Brackbill, *J. Appl. Phys.* 83 (1998) 5732.
- [22] K. Yano, Y. Horie, *Phys. Rev. B* 59 (1999) 13672.
- [23] S.I. Negreskul, S.G. Psakhie, S.Y. Korostelev, in: S.C. Schmidt, J.N. Johnson, L.W. Davison (Eds.), *Proceedings of Shock Compression of Condensed Matter*, Albuquerque, NM, North-Holland, Elsevier Science Publishers, Amsterdam, 1990, p. 233.
- [24] A.M. Renlund, J.C. Miller, W.M. Trott, K.L. Erickson, M.L. Hobbs, R.G. Schmitt, G.W. Wellman, M.R. Baer, in: *Proceedings of the 11th Symposium (International) on Detonation*, Snowmass, UT, 1998, p. 127.
- [25] B.F. Henson, R.K. Sander, S.F. Son, J.M. Robinson, P.M. Dickson, B.W. Asay, *Phys. Rev. Lett.* 82 (1999) 1213.
- [26] R. Behrens, S. Mack, J. Wood, in: *Proceedings of the 1998 JANNAF Combustion and PSHS Joint Meeting*, Tucson, AZ, 1998, p. 21.
- [27] M.R. Baer, M.L. Hobbs, R.J. Gross, R.G. Schmitt, in: *Proceedings of the 11th Symposium (International) on Detonation*, Snowmass, UT, 1998, p. 852.
- [28] V. Loyola, S. Klassen, SAND97-2721, Sandia National Laboratories, Albuquerque, NM, 1998.
- [29] J. Cesarano, M. McEuen, T. Swiler, SAND96-1703, Sandia National Laboratories, 1996.
- [30] F. van Swol, personal communication.
- [31] M. Tanemura, *Acta Stereol* 11 (1991) 41.
- [32] T.R. Gibbs, Popolato, *LASL Explosive Property Data*, University of California Press, Berkeley, 1980.
- [33] J.F. Nye, *Physical Properties of Crystals*, Clarendon Press, Oxford, 1957.
- [34] R.R. McGuire, C.M. Tarver, in: *Proceedings of the 6th Symposium (International) on Detonation*, Coronado, CA, NSWC MP 82-334, 1981, p. 56.
- [35] T.P. Russell, T.M. Allen, Y.M. Gupta, *Mater. Res. Soc. Proc.* 418 (1996) 385.
- [36] M.R. Baer, R.J. Gross, D.K. Gartling, M.L. Hobbs, in: *Proceedings of the JANNAF Propulsion System Hazards Subcommittee Meeting*, Monterey, CA, 1994.
- [37] G. I. Kerley, SAND92-0553, Sandia National Laboratories, Albuquerque, NM, 1992.
- [38] L.M. Barker, Hollenbach, *J. Appl. Phys.* 43 (1972) 4669.
- [39] D.D. Bloomquist, S.A. Sheffield, *J. Appl. Phys.* 54 (1983) 1717.
- [40] W.M. Trott, M.D. Knudson, L.C. Chhabildas, J.R. Assay, in: *Proceedings of the 1999 APS Conference on Shock Compression of Condensed Matter*, Snowbird, UT, 1999, p. 993.
- [41] W.G. Von Holle, *Fast Reactions in Energetic Systems*, Reidel Pub. Company, Preveza, Greece, 1981, p. 485.
- [42] R.E. Setchell, in: J.R. Bowen, J.C. Leyer, R.I. Soloukhin (Eds.), *Dynamics of Explosions*, AIAA, New York, 1986, p. 607.
- [43] D.J. Funk, R.L. Rabie, J.L. Mace, S. Shaw, C. Forest, V. Yuan, C. Ragan, D. Idar, L.G. Hill, D. Bowman, G. Morgan, in: *Proceedings of the 11th Symposium (International) on Detonation*, 1998, p. 45.
- [44] S.M. Sharma, Y. Gupta, Theoretical analysis of R-line shifts of ruby subjected to different deformation conditions, *Phys. Rev. B* 43 (1991) 879–893.